

# Model test and numerical analysis of active earth pressure against concrete block retaining wall

Arai, K., Machihara, H. & Lu, L.  
University of Fukui

Tsuji, S.  
Maeda Kosen Co. Ltd.

**Keywords:** active earth pressure, earth reinforcement, Mohr-Coulomb failure criterion, model test, numerical analysis

**ABSTRACT:** This paper discusses active earth pressure acting on concrete block retaining wall considering deformation and stiffness of wall and backfill material. Many laboratory model tests are performed, subjected to block retaining walls which have reinforced or non-reinforced backfill, and which have different inclination. Earth pressure distribution and active thrust, etc. are monitored according to the displacement of retaining wall. The monitored results are simulated fairly well by proposed FE analysis which employs Mohr-Coulomb yield criterion, a simple non-associated flow rule, and initial stress method for nonlinear analysis. The proposed procedure duplicates fairly well the results of full-scale model test.

## 1 INTRODUCTION

Active earth pressure acting on retaining wall is considerably influenced by the wall displacement. In spite of many conventional studies, it is difficult to duplicate the relationship between earth pressure and wall displacement. It is also difficult to estimate the earth pressure acting on concrete block retaining wall which has a backfill reinforced with geotextile, due to the complicated deformation behavior. This paper reports the result of laboratory model tests concerning concrete block retaining wall with reinforced or non-reinforced backfill, and proposes a numerical procedure which enables to simulate the results monitored in the test. For instance, the numerical analysis shows that the tensile resistance of geotextile bears horizontal shear stress within backfill soil, which may decrease the active earth pressure. The proposed procedure enables to evaluate the active earth pressure considering deformation and stiffness of reinforcement and backfill materials. It is also shown that the proposed procedure duplicates full-scale model test of reinforced retaining wall.

## 2 LABORATORY MODEL TEST

Fig. 1 shows the test equipment. Four cases of test are performed, in combination with two kinds of inclination of retaining wall in 1:0.2 and 1:0.4, and reinforced and non-reinforced backfills. In order to

eliminate the effect of friction between backfill and soil container, the backfill is constructed by heaping up aluminum sticks with 12.5mm length and 3mm and 1.6mm diameters in a ratio of 2 versus 3. Considering the scatter of backfill property due to aluminum sticks, each test case is carried out two times to obtain the average result. To stabilize the horizontal deformation of the base of backfill, a copperplate glued by aluminum stick is laid on the base. For backfill material, unit weight  $\gamma=21.7\text{kN/m}^3$ , cohesion  $c=0$  and frictional angle  $\phi=25.3^\circ$  which is calculated by averaging the angles of repose.

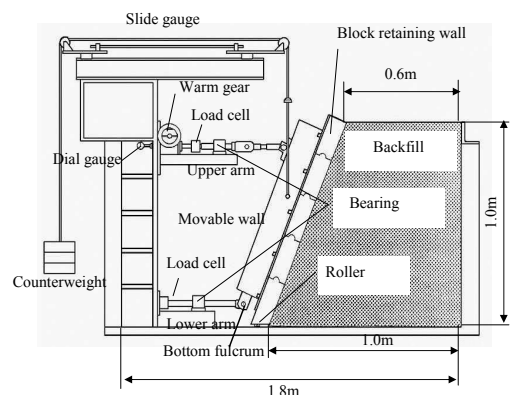


Figure 1 Test equipment

As shown in Fig. 1, we install an H-section steel bar named ‘movable wall’, which is supported by the upper and lower arms with load sensor. Because these arms are supported with ball bearing, only a horizontal force is transmitted to the load sensor. In order to cancel the dead weight of movable wall, a counterweight is installed as in Fig. 1. The movable wall is connected with the lower arm by a pin. When the worm gear on the upper arm turns, the wall rotates on the pin and the upper part of movable wall moves back smoothly due to the slide gauge shown in Fig. 1.

The segmental retaining wall (vertical height=100 cm) shown in Fig. 1 is constructed by heaping up five concrete blocks (thickness=10cm and deepness=12.5cm). In each block, a semicircular protuberance in radius of 2cm is attached on the upper side, and a semicircular groove in radius of 2.1cm is produced on the underside of block to ensure the rotation between the upstairs and downstairs blocks. In order to give smooth rotation between upper and lower blocks, a Teflon sheet is inserted between the protuberance of downstairs block and the groove of upstairs block. A roller of 2cm radius is installed on the underside of the lowest block, considering the friction between the block and the base of soil container.

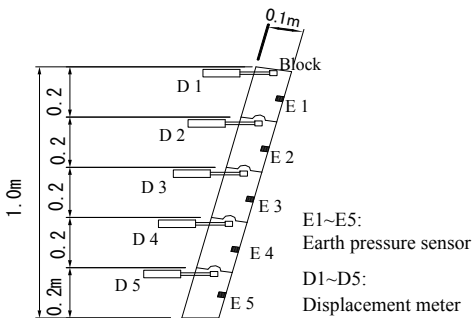


Figure 2 Layout of displacement meters and earth pressure sensors

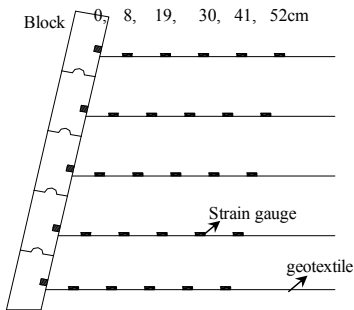


Figure 3 Configuration of instruments of geotextile

Table 1 Material properties (laboratory model test)

		Backfill	Interface
Elastic modulus	$E$ (kN/m <sup>2</sup> )	981 (active state)	981 (active state)
		9810 (static state)	9810 (static state)
Shear modulus	$G$ (kN/m <sup>2</sup> )	-	98.1
Poisson's ratio	$\mu$	0.25	0.25
Friction angle	$\varphi$ (°)	25.3	16.9
Density	$\gamma$ (kN/m <sup>3</sup> )	21.7	
		block (beam)	geotextile (truss)
Elastic modulus	$E$ (kN/m <sup>2</sup> )	$1.4 \times 10^7$	$3.9 \times 10^5$
Cross section	$A$ (m <sup>3</sup> )	0.1	0.0001
Moment of inertia	$I$ (m <sup>4</sup> )	$2.2 \times 10^{-6}$ (block)	
		$2.3 \times 10^{-9}$ (junction)	

The test equipment shown in Fig.1 is assembled as follows: 1) The movable wall is settled at the inclination constructed by the upper and lower arms. 2) Five concrete blocks are bolted on the movable wall. 3) Aluminum sticks are piled up into backfill. 4) After filling backfill, the bolts fixing the blocks on movable wall are removed. 5) Succeedingly the upper arm of movable wall moves back with the worm gear, and we measure the active thrust, earth pressure, displacement of blocks and backfill, and strains on geotextile.

The horizontal active thrust is measured by the load sensors installed on the upper and lower arms shown in Fig. 1. As shown in Fig. 2, five displacement meters are installed to measure the horizontal displacement of each concrete block. The earth pressures normally acting on the blocks are measured by the pressure sensors embedded into the groove of back of blocks. The displacement in the backfill is obtained from many markers settled in the aluminum sticks.

Five layers of geotextile (woven synthetic fiber, thickness: 0.1mm) are rigidly connected to each block, as shown in Fig. 3. Each layer of geotextile is laid in width of 12.5cm which is the same as the width of backfill soil, and extends to the edge of backfill. Fig. 3 shows the arrangement of strain gauges to measure the tensile force of geotextile. To affix the strain gauge, the geotextile is severed into five parts and joined with OHP sheet with an adhesive. The properties of geotextile are given in Table1.

### 3 NUMERICAL ANALYSIS

Fig. 4 shows the FE meshing for the equipment shown in Fig. 1. Backfill is modeled by plane strain

elements, in which stress is assumed constant. The concrete block is modeled by beam element. Interface elements are set between concrete block and backfill (Desai et al. 1984). The geotextile is represented by truss material which resists no tensile force.

When employing interface elements for both sides of concrete block, we obtain some unstable numerical results, and cannot simulate the phenomenon that the movable wall deviates from the concrete blocks. Thus the following method is employed. We have known the position of blocks separated from the movable wall from the experiment (see Fig. 8). At the lower part where the blocks do not deviate from the movable wall, a high bending stiffness is given to the beam element of blocks. At the upper part where the blocks deviate from the movable wall, an extremely low bending stiffness is assumed to the junction between upper and lower blocks to represent the rotation of blocks.

The upper active thrust is monitored at the upper arm of movable wall, whereas the actual upper load acts on the block at the position where the movable wall deviates from the blocks. In the numerical analysis, the upper load from the movable wall acts on the position of separation, and 'value of upper load sensor:  $F_e$ ' and 'horizontal displacement of movable wall at the upper arm:  $D_e$ ' are calculated as

$$F_e \times L_a = F_n \times L_d \quad (1)$$

$$D_e; L_a = D_n; L_d \quad (2)$$

where,  $L_a$ : distance between the upper arm and the bottom fulcrum,  $F_n$ : upper load obtained from the numerical analysis,  $L_d$ : distance between the bottom fulcrum and the position of the blocks away from the movable wall, and  $D_n$ : horizontal displacement at the upper load point.

Since numerical computation becomes unstable when considering the interface elements above and below the geotextile, we do not put these interface elements.

The numerical steps are as follows. 1) Establishing the concentrated load  $F_e$  toward the upper arm. 2) According to Eq. (1), converting  $F_e$  into  $F_n$ , and then employing the FE analysis in which the load is taken as the aggregate of the  $F_n$  and the unit weight of backfill. 3) Calculating the value of  $D_e$  from the results at step 2), and then understanding the relationship between earth pressure and rear displacement of movable wall in the upper arm. 4) The computation corresponding to the load applied on the upper arm is performed independently of the each stage of load.

Mohr-Coulomb  $F_M$  and Coulomb  $F_C$  failure criteria are employed respectively to backfill and interface. As shown in Fig. 5, when applying further confining pressure after yield point A, the stress state is assumed to move along the yield surface. At the

elasto-plastic state from point A to B, we employ a simple non-associated flow rule as shown in Fig. 5. The backfill is assumed to bear no tensile stress, and reinforcement material is assumed to sustain no compressive force.

We evaluate the stability analysis of geotechnical structure mainly by its final state as in the limit equilibrium analysis. The distribution of yield elements calculated by the initial stress method is relatively accordance with the final collapse pattern. Two types of nonlinearity (nonlinear stress-strain relationship and no tension) are well treated by the original initial stress method (Zienkiewicz et al. 1968, 1969). The details are given by Arai (1993).

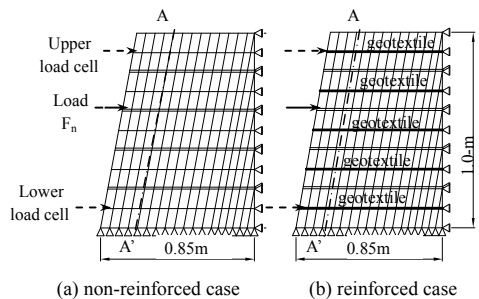


Figure 4 FE meshing

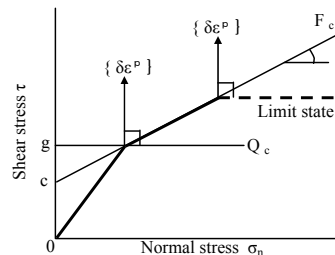


Figure 5 Failure criterion and flow rule (Coulomb material)

#### 4 ANALYTICAL AND TEST RESULTS

Table 1 lists the material parameters, where E: Young's modulus,  $\mu$ : Poisson's ratio, G: shear modulus of interface,  $\gamma$ : unit weight, A: cross area, and I: moment of inertia. The  $\phi$  and  $\gamma$  are obtained from tests. Since the elastic modulus has little influence to active thrust, we give a standard value. The stiffness of concrete block is taken as the minimum bending stiffness within the limits of no displacement. Subjected to the conjugation part between the upper and lower blocks, we take 1/10 of bending stiffness of concrete block. The elastic modulus of geotextile is determined by a tensile test.

Fig. 6 shows the calculated displacement of backfill when the rear displacement of movable wall is 16mm, where the settlement due to the own weight of backfill is also included. The horizontal displacement of backfill with geotextile is smaller than the result without geotextile, which is a fairly good agreement with the test result. Almost backfill elements have yielded irrelative of the usage of geotextile and the inclination of retaining wall.

Fig. 7 shows the monitored relationship between horizontal displacement of concrete blocks and rear displacement of movable wall. When the former is proportional to the latter, the block and the movable wall are regarded as united. The block is separated from the movable wall in a sudden turn for the displacement of block. The displacement for reinforced backfill is smaller than that for non-reinforced case. The displacement of fifth layer of block (nethermost block) is restricted due to its position near the bottom fulcrum of movable wall. Fig. 8 shows the distribution of horizontal displacement. The movable wall is rigid body and rotates on the bottom fulcrum. The displacements of blocks and movable wall agree almost before the blocks separated from the wall. In Fig. 8, for the non-reinforced case, the uppermost block is separated from the movable wall for the inclination of 1:0.2. For the reinforced case, many blocks are separated, because the displacement is restrained by geotextile. The calculated results duplicate fairly well the observed results. In the experiment, a Teflon sheet between the upper and lower blocks decreases the friction between the two blocks and reduces the bending stiffness. Since the numerical analysis gives a little larger bending stiffness, the calculated displacement is smaller than the monitored one after the blocks has separated from the movable wall.

Fig. 9 shows the distribution of horizontal earth pressure. Since the normal earth pressure is actually monitored in the back of block, the horizontal earth pressure  $p$  is calculated by

$$p = p_N \cos(\delta + \omega - 90^\circ) / \cos \delta \quad (3)$$

where,  $p_N$ : earth pressure measured,  $\delta$ : internal friction angle between blocks and backfill ( $2\phi/3$ ),  $\omega$ : initial inclination of block retaining wall. As in Fig. 9, the results of earth pressure disperse in a certain degree, due to the effect of piling method of aluminum sticks. Except the nethermost block, the earth pressure decreases with the rear displacement of movable wall and gradually becomes a constant value. Fig. 10 shows that the distribution of horizontal earth pressure decreases with the rear displacements. For non-reinforced case, the monitored and calculated earth pressures for 16mm rear displacement give the approximate value with the Coulomb solution which assumes the triangular distribution. As shown in Fig. 1, due to the center of the nethermost block as the fulcrum of movable wall, this block ro-

tates on the fulcrum to generate the passive earth pressure when the movable wall moves backward. For the reinforced case, the monitored and calculated results are different from the Coulomb solution. As in Fig. 10(b), the calculated earth pressure for 16mm rear displacement approaches zero because the block is separated from the movable wall. The calculated earth pressure after the movable wall departs from the block is less than the monitored result. In the experiment, a Teflon sheet between the upper and lower blocks reduces the friction with the rotation of the blocks. The separated block leans toward the backfill in the own weight, which may yield a certain amount of earth pressure. In the analysis, because a slight rigidity exists in the junction, the separated block is independent of the movable wall and then the pressure to the backfill is reduced. This may be one of the reasons why the calculated earth pressure is lower than the Coulomb solution.

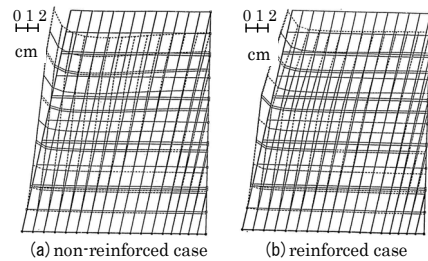
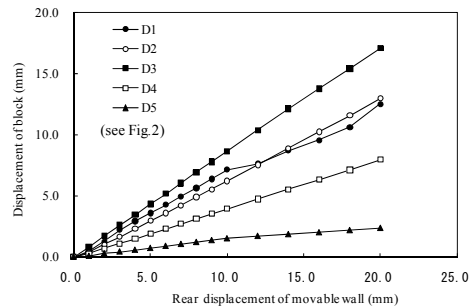
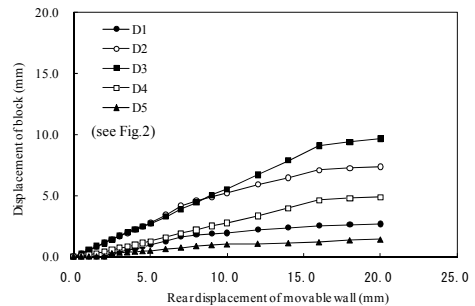


Figure 6 Displacement of backfill (analytical results)



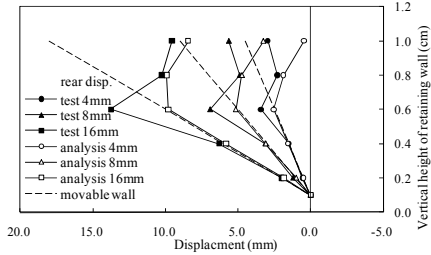
(a) non-reinforced case



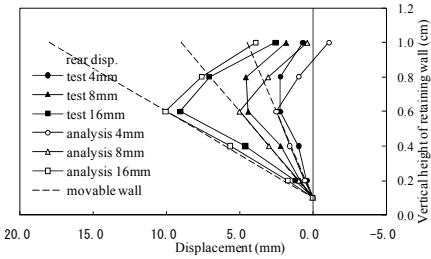
(b) reinforced case

Figure 7 Horizontal displacement of block (test results, backfill inclination of 1:0.2)

The monitored horizontal active thrust is obtained by the sum of the upper and lower load sensors shown in Fig. 1. It is also possible to estimate the active thrust from the measured earth pressure. Since the measured earth pressure tends to include some errors stated previously, we select the active thrust obtained from the load sensors as the measured value.

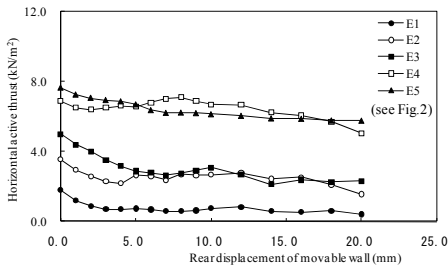


(a) non-reinforced case

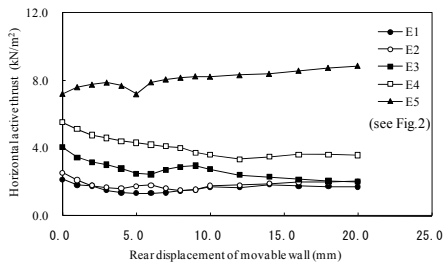


(b) reinforced case

Figure 8 Distribution of horizontal displacement of block (backfill inclination of 1:0.2)

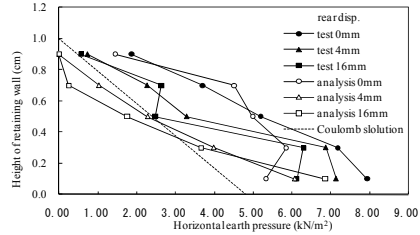


(a) non-reinforced case

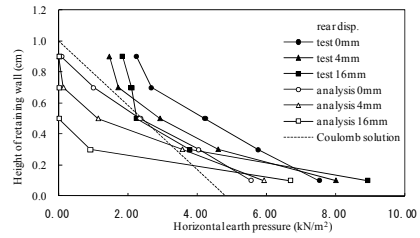


(b) reinforced case

Figure 9 Horizontal earth pressures (backfill inclination of 1:0.2)

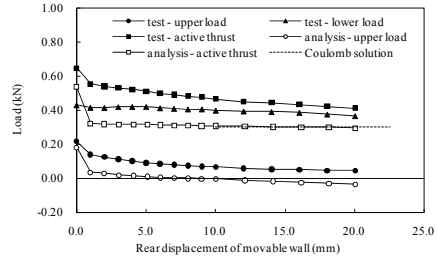


(a) non-reinforced case

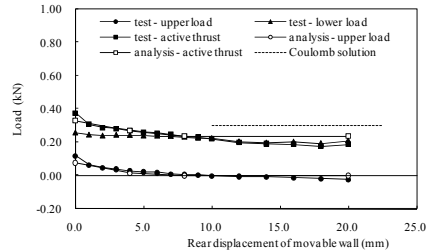


(b) reinforced case

Figure 10 Distribution of horizontal earth pressures (test results, backfill inclination of 1:0.2)



(a) non-reinforced case



(b) reinforced case

Figure 11 Horizontal active thrust (backfill inclination of 1:0.2)

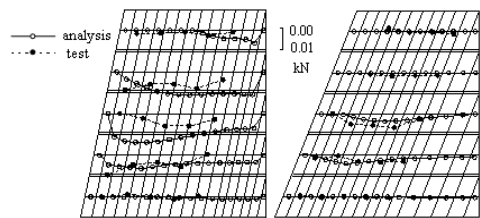
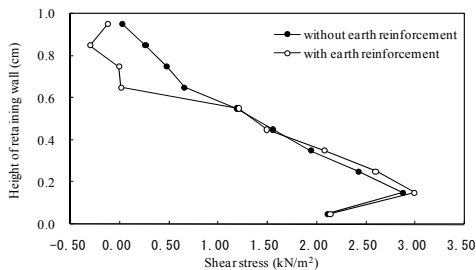


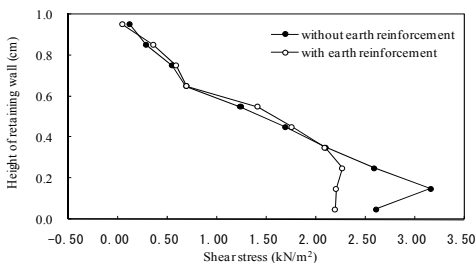
Figure 12 Tensile forces on earth reinforcement (16mm rear displacement of movable wall)

Fig. 11 compares the monitored and calculated results of horizontal active thrust. The calculated active thrust is obtained from the horizontal component of normal and shear stresses on the interface element between the blocks and backfill. As in Fig. 11, the active thrust decreases with the rear displacement of movable wall, and approaches constant over 10mm rear displacement into full active state. Except the non-reinforced backfill in the inclination of 1:0.2, the upper load sensor gets the minus value with the rear displacement. Moving away from the movable wall, the upper block is no longer supported by the wall. Thus the tensile force works at the upper load sensor. In any inclination, the calculated results are close to the monitored those irrelative of using geotextile. In the non-reinforced backfill, both the analysis and experiment provide the approximate result with the Coulomb solution. For the reinforced backfill, the calculated and monitored results are lower than the Coulomb solution.

Fig. 12 shows the monitored and calculated tensile force acting on the geotextile. There is small difference between the monitored and calculated results, whereas a general tendency is similar. The difference may be due to the limitation of the measured technique of tensile force on geotextile. The tensile force in the inclination of 1:0.2 is generally larger than that of 1:0.4, because the geotextile give full play for the former case. Both cases show that the position of maximum tensile force is not directly related to the position of slip surface estimated from the deformation of backfill.



(a) inclination of 1:0.2



(b) inclination of 1:0.4

Figure 13 Distribution of shear stress in backfill (4mm rear displacement of movable wall)

Fig. 13 shows the shear stress distribution of A-A' or B-B' section of backfill (see Fig. 4) for the rear displacement of movable wall is 16mm. In the upper part of backfill in the inclination of 1:0.2, the shear stress for the reinforced case is smaller than that for the non-reinforced case. The large tensile force is seen in the upper part of backfill referred to Fig. 12(a). On the other hand, in the inclination of 1:0.4, the shear stress for the reinforced case is smaller than that the non-reinforced case in the lower part of backfill. The large tensile force is seen in the middle and lower part of backfill from Fig. 12(b). The horizontal and vertical stresses are independent on the inclination of backfill and the use of geotextile. The shear strain in the backfill is reduced by the horizontal tensile force given by geotextile, which decreases the horizontal active thrust acting on the retaining wall. This is a complicated phenomenon which is dependent on the variation of stress distribution of backfill with the inclination of retaining wall, and which is influenced by the stiffness and strength of backfill and geotextile. It may be difficult to simply and practically indicate this phenomenon by means other than the numerical procedure.

## 5 CONCLUSIONS

Based on a laboratory model test, this paper proposed a numerical procedure to calculate the active earth pressure acting on the concrete block retaining wall reinforced by geotextile. The procedure enables to take stiffness and deformation of material into consideration. The results monitored in the model tests, are simulated fairly well by the proposed procedure. The numerical result shows that the geotextile bears some parts of shear stress in backfill due to its tensile resistance. This mechanism reduces the earth pressure in reinforced retaining wall structure.

## REFERENCES

Arai, K. 1993. Active earth pressure founded on displacement field. *Soils and Foundations*, Vol. 33, No. 3, pp. 54-67.  
 Desai, C.S., Zaman, M.M. Lightner, J. G. & Siriwardane, H. J. 1984. Thin-layer element for interfaces and joints. *Int. J. Numer. Anal. Methods Geomech*, Vol. 8, pp. 19-43.  
 Zienkiewicz O. C., Valliappan S., King I. P. 1968. Stress analysis of rock as a 'no tension material'. *Géotechnique*, Vol. 18, pp. 56-66.  
 Zienkiewicz O. C., Valliappan S., King I. P. 1969. Elastoplastic solutions of engineering problems 'initial stress', finite element approach. *International Journal for Numerical Methods in Engineering*, Vol. 1, pp. 75-100.